



# Stratifin regulates stabilization of receptor tyrosine kinases via interaction with ubiquitin-specific protease 8 in lung adenocarcinoma

Yunjung Kim<sup>1</sup> · Aya Shiba-Ishii<sup>1</sup> · Tomoki Nakagawa<sup>2</sup> · Shun-ichiro Iemura<sup>3</sup> · Tohru Natsume<sup>4</sup> · Noriyuki Nakano<sup>1</sup> · Ryota Matsuoka<sup>1</sup> · Shingo Sakashita<sup>1</sup> · SangJoon Lee<sup>5</sup> · Atsushi Kawaguchi<sup>6</sup> · Yukio Sato<sup>7</sup> · Masayuki Noguchi<sup>1</sup>

Received: 10 December 2017 / Revised: 9 April 2018 / Accepted: 10 May 2018 / Published online: 7 June 2018  
© Macmillan Publishers Limited, part of Springer Nature 2018

## Abstract

Previously we have reported that stratifin (SFN, 14-3-3 sigma) acts as a novel oncogene, accelerating the tumor initiation and progression of lung adenocarcinoma. Here, pull-down assay and LC-MS/MS analysis revealed that ubiquitin-specific protease 8 (USP8) specifically bound to SFN in lung adenocarcinoma cells. Both USP8 and SFN showed higher expression in human lung adenocarcinoma than in normal lung tissue, and USP8 expression was significantly correlated with SFN expression. Expression of SFN, but not of USP8, was associated with histological subtype, pathological stage, and poor prognosis. USP8 stabilizes receptor tyrosine kinases (RTKs) such as EGFR and MET by deubiquitination, contributing to the proliferative activity of many human cancers including non-small cell lung cancer. In vitro, USP8 binds to SFN and they co-localize at the early endosomes in lung adenocarcinoma cells. Moreover, USP8 or SFN knockdown leads to downregulation of tumor cellular proliferation and upregulation of apoptosis, p-EGFR or p-MET, which are related to the degradation pathway, and accumulation of ubiquitinated RTKs, leading to lysosomal degradation. Additionally, mutant USP8, which is unable to bind to SFN, reduces the expression of RTKs and p-STAT3. We also found that interaction with SFN is critical for USP8 to exert its autodeubiquitination function and avoid dephosphorylation by PP1. Our findings demonstrate that SFN enhances RTK stabilization through abnormal USP8 regulation in lung adenocarcinoma, suggesting that SFN could be a more suitable therapeutic target for lung adenocarcinoma than USP8.

## Introduction

The most common histological type of lung cancer is adenocarcinoma [1], categorized as non-small cell lung cancer (NSCLC), which has a 5-year survival rate of approximately 40%. However, Noguchi et al. have demonstrated that adenocarcinoma in situ (AIS, type A and B in the Noguchi classification) has an extremely favorable

---

These authors contributed equally: Yunjung Kim, Aya Shiba-Ishii

**Electronic supplementary material** The online version of this article (<https://doi.org/10.1038/s41388-018-0342-9>) contains supplementary material, which is available to authorized users.

✉ Aya Shiba-Ishii  
aya\_shiba@md.tsukuba.ac.jp  
✉ Masayuki Noguchi  
nmasayuk@md.tsukuba.ac.jp

<sup>1</sup> Department of Pathology, Faculty of Medicine, University of Tsukuba, Ibaraki, Japan

<sup>2</sup> Doctoral Program in Biomedical Sciences, Graduate School of Comprehensive Human Sciences, University of Tsukuba, Ibaraki, Japan

<sup>3</sup> Translational Research Center, Fukushima Medical University,

Fukushima, Japan

<sup>4</sup> Molecular Profiling Research Center for Drug Discovery, National Institutes of Advanced Industrial Science and Technology, Tokyo, Japan

<sup>5</sup> Ph.D. Program in Human Biology, School of Integrative and Global Majors, University of Tsukuba, Ibaraki, Japan

<sup>6</sup> Department of Infection Biology, Faculty of Medicine, University of Tsukuba, Ibaraki, Japan

<sup>7</sup> Department of Thoracic Surgery, Faculty of Medicine, University of Tsukuba, Ibaraki, Japan

outcome, with a 5-year survival rate of 100% [2]. AIS shows stepwise progression to early but invasive adenocarcinoma (eIA, type C in the Noguchi classification), which has a relatively poorer outcome [3]. Previously, we compared the gene expression profiles of eIA and AIS and found that stratifin (SFN, 14-3-3 sigma) shows significantly higher expression in eIA than in AIS. This led us to conclude that SFN facilitates the development of lung adenocarcinoma and progression *in vivo* [4, 5].

SFN is the most distinct member of the highly conserved 14-3-3 protein family, which includes the beta, epsilon, eta, gamma, tau, zeta, and sigma forms [6]. Although each of the 14-3-3 proteins has unique tissue-selective functions, SFN is the form most directly related to tumor progression in the lung [7, 8]. SFN acts as an adapter protein that controls signal transduction, protein trafficking, the cell cycle, and apoptosis [9] by binding to a specific phosphoserine/threonine-containing motif on various proteins [7]. This interaction is generally phosphorylation dependent on the target protein regulated by kinases such as AKT and phosphatases such as PP1 and PP2A [10]. On the basis of the existing evidence, we hypothesized that the functions of SFN and its binding partners might be of special relevance to lung adenocarcinoma and associated with its stepwise progression. To clarify the molecular mechanism whereby SFN might facilitate tumor progression, we performed a pull-down assay and LC-MS/MS analysis using a lung adenocarcinoma cell line (A549) and identified ubiquitin-specific protease 8 (USP8) as a lung adenocarcinoma-specific binding partner of SFN.

USP8 belongs to the ubiquitin-specific protease (USP) superfamily of deubiquitinating enzymes (DUBs) that stabilize specific protein substrates by removing ubiquitin from them [11]. USP8 has already been reported to target several particular substrates, including smoothened [12], frizzled [13], neuregulin receptor degradation protein-1 (Nrdp1) [14], and receptor tyrosine kinases (RTKs) [15–17], which are involved in a number of human diseases including malignant neoplasms, to balance their lysosomal degradation [15, 18]. However, the mechanism responsible for controlling the deubiquitination activity of USP8 is still poorly understood. Among the various targets of USP8, RTKs such as epidermal growth factor receptor (EGFR) and hepatocyte growth factor receptor (MET) are the best-known therapeutic targets in lung cancer [19]. Moreover, our recent study has demonstrated that overexpression of USP8 in lung adenocarcinoma was related to the expression and mutation status of EGFR and evident even in AIS, an early stage of lung adenocarcinoma [20].

On the other hand, our previous immunohistochemical study showed that normal lung tissues were completely negative for SFN, whereas most cases of invasive lung adenocarcinoma showed SFN positivity, indicating that SFN expression has high tumor selectivity [4]. If SFN regulates

USP8 activity in a tumor-selective manner, then SFN might be a better therapeutic target than USP8 to facilitate RTK degradation. Interestingly, two independent groups have reported somatic mutation at the 14-3-3 binding motif (RSYSSP) of USP8 in patients with Cushing's disease [21, 22]. However, this genetic alteration and its implications in lung adenocarcinoma have not been clarified.

In the present study, we investigated the molecular mechanism underlying the binding of SFN to USP8 in lung adenocarcinoma cells because the role of this interaction in RTK stabilization was considered a promising avenue for identifying a useful therapeutic target for lung adenocarcinoma.

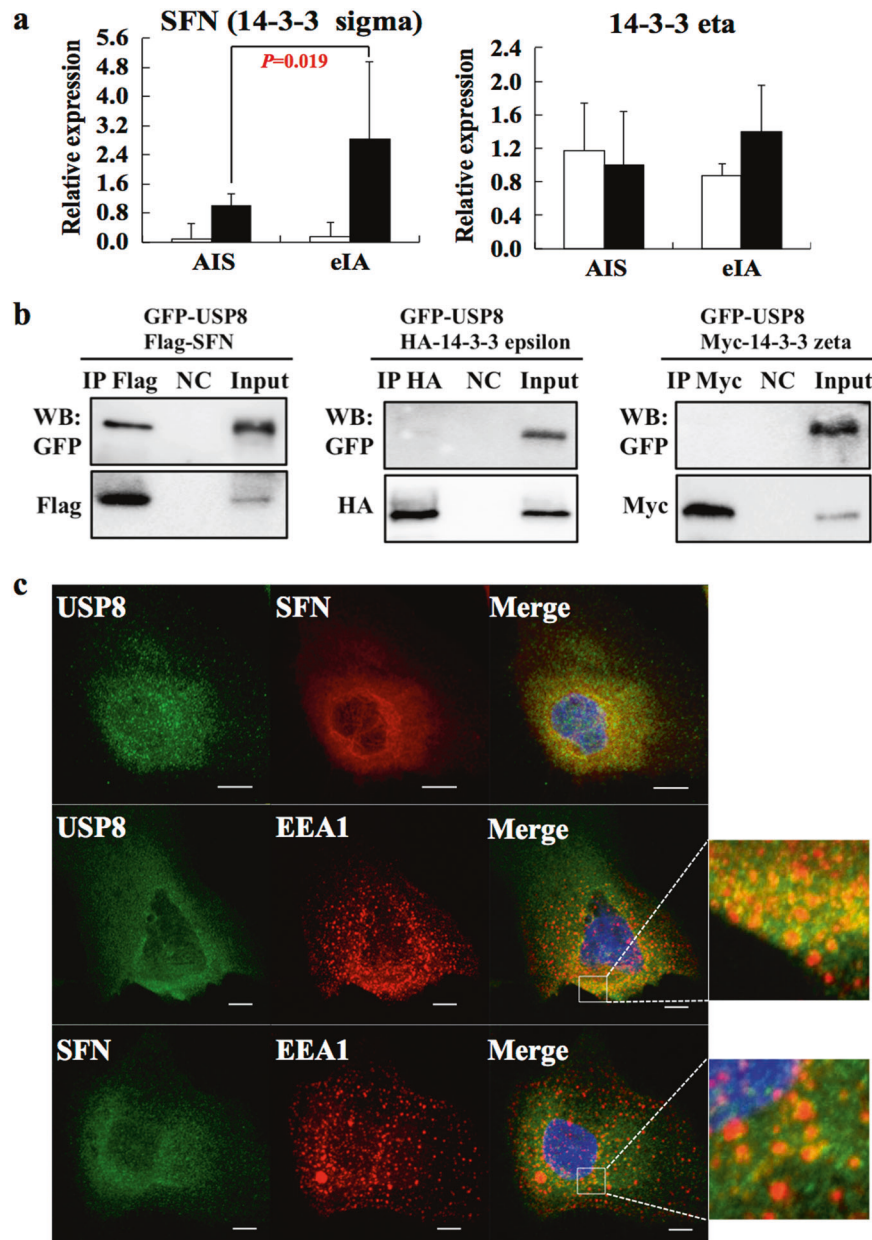
## Results

### Identification of USP8 as a unique SFN binding partner in lung adenocarcinoma cells

Expression analysis of the 14-3-3 family revealed that all members other than SFN showed no difference in mRNA expression among eIA, AIS, and normal lung tissue (Fig. 1a and Supplementary Fig. S1a). Therefore, we speculated that only SFN specifically accelerated the progression of lung adenocarcinoma, and attempted to screen factors that bind specifically to SFN but not to other 14-3-3 members. To identify SFN binding partners in lung adenocarcinoma cells, we subjected A549 cells transfected with SFN or 14-3-3 eta (as a control) vectors to a pull-down assay and LC-MS/MS analysis. On the basis of the results, 24 proteins showed an association with SFN only, and not with 14-3-3 eta (Supplementary Table S1). Among the candidate proteins, we focused on USP8 as a direct binding partner of SFN. In addition, we detected endogenous interaction between USP8 and SFN in A549 cells, but not USP8 and 14-3-3 eta. (Supplementary Fig. S1b).

Previous studies have found that USP8 interacts with 14-3-3 proteins in embryonic murine brain [23] and T-cells [24], but not in lung. To clarify whether USP8 binds specifically to SFN in lung adenocarcinoma, we carried out coimmunoprecipitation (co-IP) to examine the interaction of USP8 with SFN, 14-3-3 epsilon, or 14-3-3 zeta, separately. Unlike previous observations [21, 25, 26], the results indicated that among three kinds of 14-3-3 proteins, only SFN bound specifically to USP8 in PL16T, an immortalized AIS cell line [27] (Fig. 1b). In addition, immunofluorescence (IF) showed that USP8 and SFN were co-localized in the cytoplasm, particularly in early endosomes, where USP8 predominantly controls lysosomal degradation of target proteins, such receptors at plasma membrane (Fig. 1c). These data indicated that USP8 specifically interacts with SFN and they co-localize in early endosomes.

**Fig. 1** USP8 specifically interacts with SFN at the endosomes. **a** Real time RT-PCR of SFN (14-3-3 sigma) and 14-3-3 eta using frozen tissues of lung adenocarcinoma. Ten paired specimens of tumor and adjacent normal lung tissue were used. The white bar indicates normal tissue, and the black bar, tumor tissue. AIS: adenocarcinoma in situ; eIA: early invasive adenocarcinoma. **b** PL16T cells were transfected with various plasmids for 24 h to investigate the interaction between USP8 and 14-3-3 proteins (HA-epsilon: HA tagged 14-3-3 epsilon and Myc-zeta: Myc tagged 14-3-3 zeta). Co-IP was performed using the indicated antibodies. Only SFN showed binding with USP8. **c** Localization of endogenous USP8 and SFN was examined by IF. EEA1 was used as an early endosome marker. SFN and USP8 showed co-localization at the early endosomes. Quantitative determination of each fluorescent signal (SFN or USP8: green and EEA1: red) was performed along the white arrows shown inside the images. The Y-axis indicates the fluorescence pixel intensity, demonstrating a distinct association between SFN and EEA1 or USP8 and EEA1. Scale bars, 10  $\mu$ m



### USP8 and SFN are highly expressed in human lung adenocarcinoma tissues

To evaluate the expression of USP8 and SFN in human lung adenocarcinoma tissues, we performed immunohistochemistry (IHC) using 193 lung adenocarcinoma cases. Similarly to the results of IF, we observed that both USP8 and SFN were stained in the cytoplasm of formalin-fixed paraffin-embedded (FFPE) specimens from surgically resected lung adenocarcinoma and that the expression was higher in tumor tissue than in normal lung tissue (Fig. 2a). Additionally, we validated the results of IHC by Western blotting using paired fresh human lung tissue samples from six patients (Fig. 2b). In IHC, USP8 and SFN showed similar

expression patterns, and their expression was significantly correlated in 144/193 cases (74.6%, Fig. 2c).

Moreover, we found that SFN expression was significantly associated with sex, pathological subtype, pathological stage, lymphatic permeation, and vascular invasion (Supplementary Table S2). Unlike SFN, USP8 expression was significantly associated with only the Noguchi classification for small adenocarcinomas of the lung (2 cm or less in diameter) (Supplementary Table S2). Furthermore, SFN positivity was significantly associated with a poorer outcome relative to SFN-negative cases ( $P = 0.007$ , Fig. 2d), whereas USP8 positivity was not ( $P = 0.974$ , Fig. 2e). To interpret the different association on patient's outcome between SFN and USP8, which have

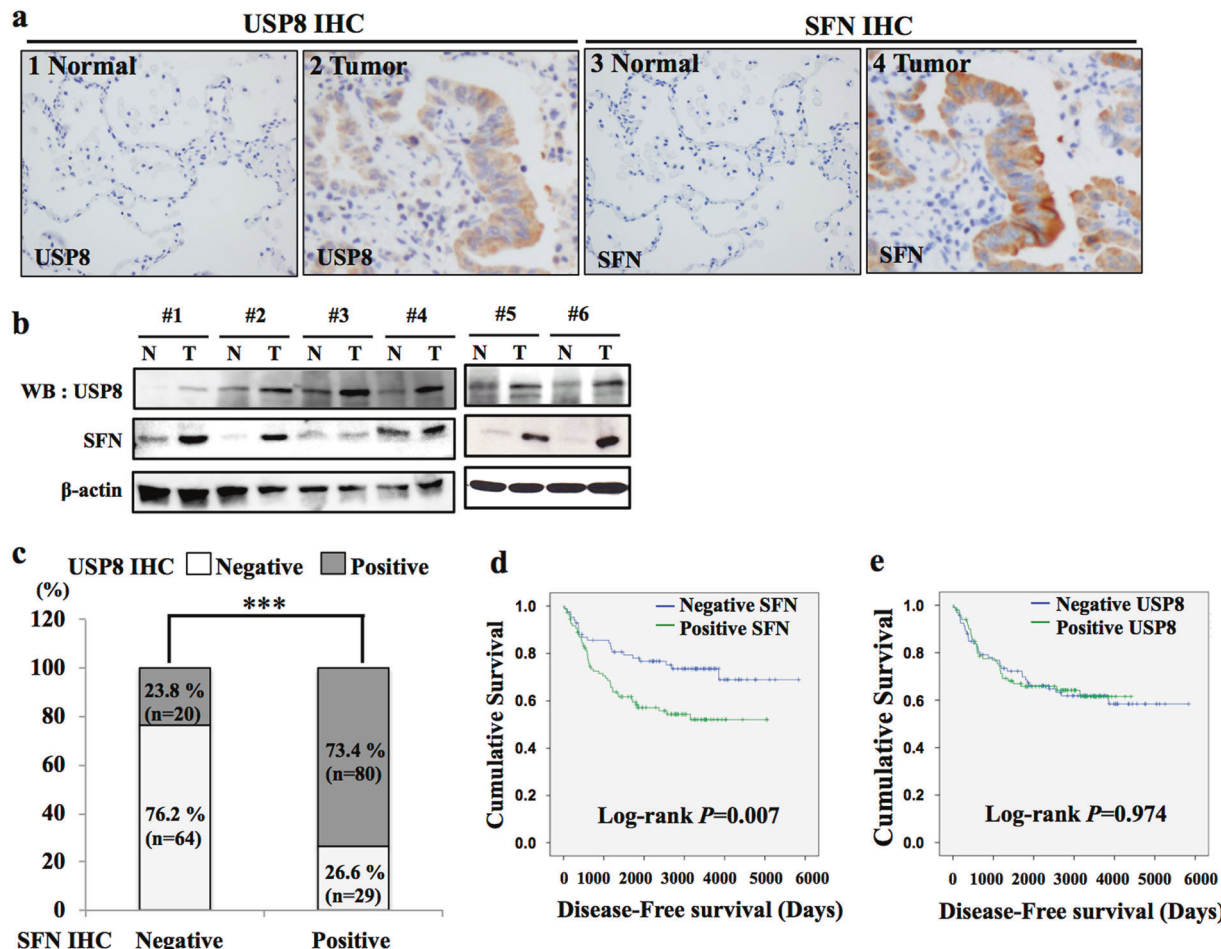


**Fig. 2** USP8 and SFN show a corresponding increase of expression in human lung adenocarcinoma tissue. **a** IHC for USP8 and SFN was performed using FFPE specimens of 193 cases of surgically resected lung adenocarcinoma. USP8 and SFN were detected mainly in the cytoplasm of the tumor cells with a similar staining pattern. Normal lung tissue was almost negative for USP8 and SFN, whereas tumor tissue showed higher expression of USP8 and SFN. **b** Western blotting of six paired specimens of fresh normal and tumor lung tissue demonstrated expression of USP8 and SFN. Both proteins expressions

were higher in tumorous than in normal tissue. **c** Correlation analysis of USP8 and SFN was performed using the IHC results. There were significantly more correlated cases than uncorrelated cases in USP8 and SFN IHC (chi-squared test, \*\*\* $P < 0.001$ ). **d**, **e** Disease-free survival depicted as Kaplan-Meier curves showing the correlation between outcome and SFN or USP8 expression. Positive expression of SFN was associated with a poorer outcome than was negative expression ( $P = 0.007$ ), but this was not the case for USP8 expression ( $P = 0.974$ )

mutually correlated expression, all patients were divided into USP8 negative and positive groups, and then patient's outcome for each group was analyzed with SFN expression. Even in the patients group with USP8 negativity, SFN positive patients showed significantly poorer outcome relative to SFN-negative cases (Supplementary Fig. S2).

### Knockdown of USP8 and SFN decreases cellular proliferation and induces apoptosis in lung adenocarcinoma cells

To examine siRNA targeting USP8 or SFN for functional analysis, we transfected with three different kinds of

siRNA-USP8 or SFN into the A549 cells that we had used for the pull-down assay and LC-MS/MS analysis. All of the siRNAs successfully suppressed the expression of USP8 or SFN mRNA and protein in A549. As siUSP8-I or siSFN-I showed the strongest suppression of cellular proliferation, we selected it and used it for further analysis (Fig. 3a–f).

To evaluate whether USP8 and SFN regulate cellular functions including cell growth, proliferation, and apoptosis, we transfected siRNA-USP8, SFN, or a scrambled control (siCON) into lung adenocarcinoma cells. Knockdown of USP8 or SFN significantly reduced the cell growth and proliferation of all lung adenocarcinoma cell lines (Fig. 3g, h). In addition, by examining the resulting alteration of a representative apoptotic protein, cleaved caspase 3, by

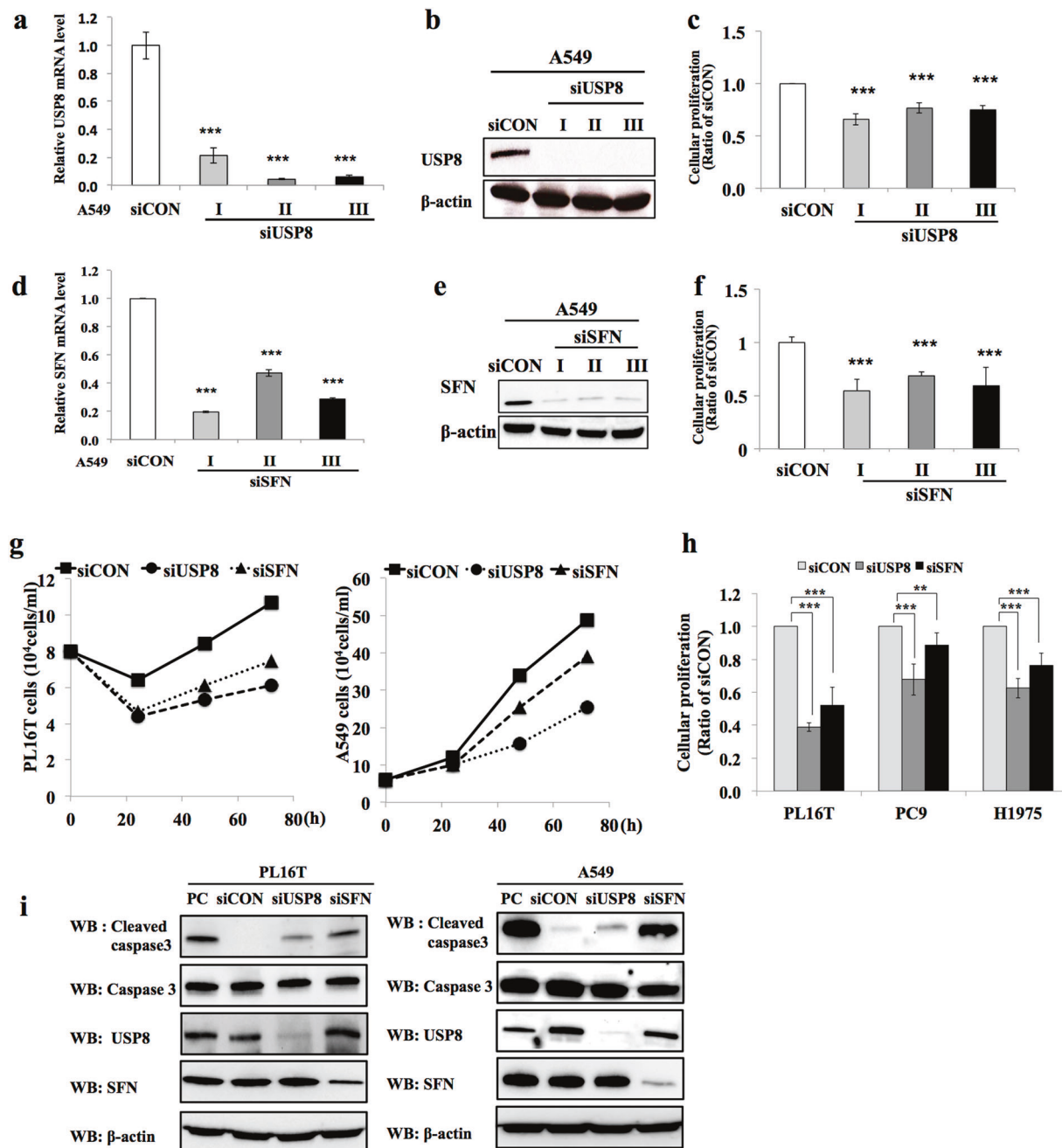
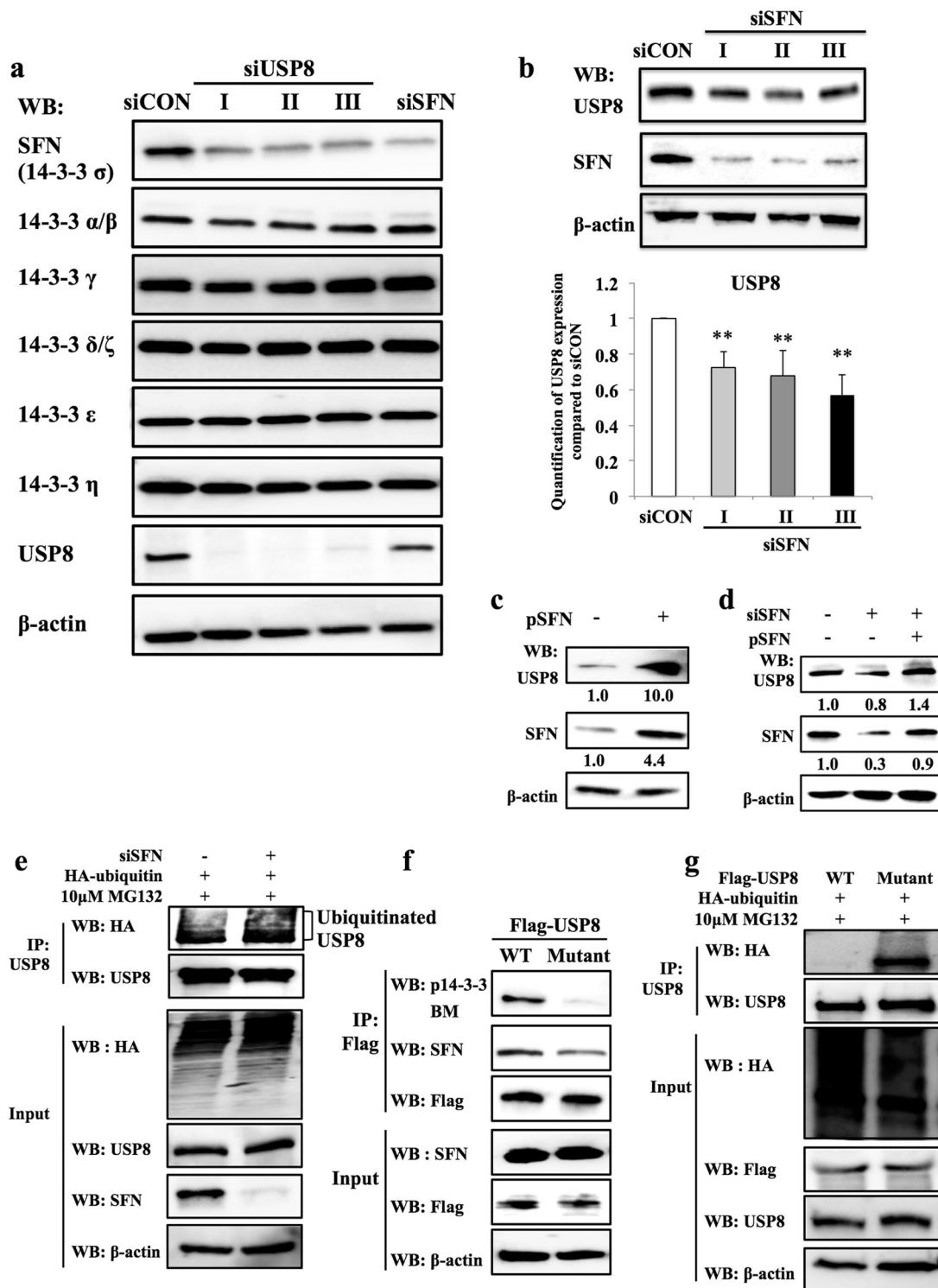


**Fig. 3** Knockdown of USP8 and SFN regulates proliferation and apoptosis in lung adenocarcinoma cells. A549 was transfected with three kinds of siRNA-USP8 or siRNA-SFN. Knockdown efficiency was confirmed at the mRNA and protein levels. **a, d** Total RNA was extracted from the cells after siRNA transfection for 24 h. USP8 and SFN mRNA were examined by real-time RT-PCR, and 18 S was used as an internal control ( $n = 3$ ,  $t$  test  $***P < 0.001$ ). **b, e** Total protein was extracted from the cells after siRNA transfection for 48 h. USP8 and SFN protein were subjected to Western blotting.  $\beta$ -actin was used as a control to verify equal loading of protein (20  $\mu$ g). **c, f** Cellular proliferation was examined using a WST-1 assay after siRNA transfection for 48 h ( $n = 12$ ,  $t$  test  $***P < 0.001$ ). Among the three siRNA

sequences, the most effective siRNA-USP8-I and -SFN-I were selected for further analysis. **g** Cell growth was examined after siRNA transfection into PL16T and A549 at the indicated time periods. Cells were counted with a hemacytometer ( $n = 3$ ). **h** Cellular proliferation was tested using the AIS cell line, PL16T, and the adenocarcinoma cell lines, PC9 and H1975 ( $n = 12$ ,  $t$  test  $**P < 0.01$ ,  $***P < 0.001$ ). **i** Expression of caspase 3 and cleaved caspase 3 as representative apoptosis-related proteins was analyzed using extracted total protein after collecting both adherent and floating cells for 48 h after siRNA transfection into PL16T and A549. The positive control was pretreated with 10  $\mu$ M camptothecin for 24 h at 37 °C in a 5% CO<sub>2</sub> incubator before protein extraction



Western blotting, we found that knockdown of USP8 or SFN also led to induction of apoptosis in both PL16T and A549 (Fig. 3i). Taken together, our results showed that USP8 and SFN are involved in cellular proliferation and apoptosis in lung adenocarcinoma cells.

### SFN regulates USP8 protein expression in AIS cells

On the basis of the specific interaction between USP8 and SFN among the other 14-3-3 members in lung adenocarcinoma cells, we speculated that USP8 and SFN might

**Fig. 4** USP8 and SFN mutually regulate their stabilization in lung adenocarcinoma cells. **a** Expression of 14-3-3 proteins was assessed by Western blotting using PL16T cells transfected with siUSP8. **b** Expression of USP8 was assessed by Western blotting using PL16T cells transfected with siSFN. We performed three independent experiments and quantified each band size to show USP8 expression using a bar graph. **c** The SFN plasmid without a tag to prevent any interruption of its interaction with target proteins was transfected into cells 24 h before protein extraction. Expression of USP8 and SFN was examined by Western blotting. **d** USP8 rescue assay was performed by Western blotting under cotransfection with siSFN for 24 h and subsequent overexpression of siSFN-resistant SFN for 24 h. **e** Expression of ubiquitinated USP8 was assessed by co-IP after transfection with siSFN accompanying overexpression of HA-ubiquitin in A549 cells. The cells were treated with 10 μM MG132 (a proteasome inhibitor) for 16 h, leading to accumulation of ubiquitinated USP8 in the proteasomes. **f** Mutant USP8 S718C contained a point mutation changing serine to cysteine at amino acid residue 718, which is one of the important phosphorylation site of the 14-3-3 binding motif (AA715-720, RSYSSP) in USP8. A549 cells transfected with WT or mutant (S718C) USP8 were tested for their interaction with SFN by co-IP. p14-3-3 BM (phospho-14-3-3 binding motif) indicates the active form of USP8 (phospho-USP8). **g** Autodeubiquitination activity was examined after overexpression of WT or mutant (S718C) USP8 in the presence of 10 μM MG132 for 16 h in A549 cells. β-actin was used as a control to verify equal loading of protein (20 μg)

mutually influence their respective stability. As expected, knockdown of USP8 reduced only SFN expression, but not that of other 14-3-3 members (Fig. 4a), indicating that USP8 stabilizes SFN in lung adenocarcinoma cells. Moreover, knockdown of SFN also significantly decreased the expression of USP8 (Fig. 4b), and conversely, overexpression of SFN increased the expression of USP8 (Fig. 4c). To confirm the direct regulatory effect of SFN on USP8 expression, we performed a rescue experiment and found that the reduction of USP8 expression after SFN knockdown was abrogated by overexpression of siSFN-resistant SFN (Fig. 4d).

Next, to investigate whether SFN regulates the stability of USP8, we examined ubiquitinated USP8 after knockdown of SFN in A549. Knockdown of SFN increased the expression of ubiquitinated USP8, indicating that SFN is able to stabilize USP8 in lung adenocarcinoma (Fig. 4e). We then considered how SFN might regulate USP8 stabilization. It is possible that USP8 exerts its self-ubiquitin remodeling function through autodeubiquitination activity, similarly to USP19 [28]. To test this hypothesis, we first generated a mutant form of USP8, S718C, harboring a point mutation at S718 of the 14-3-3 binding motif (14-3-3 BM) in USP8. We performed co-IP after overexpression of either wild-type (WT) or mutant USP8 (S718C), and interaction of the mutant USP8 (S718C) with SFN was found to be obstructed (Fig. 4f). We then examined ubiquitinated USP8 in the presence of MG132, a protease inhibitor. The ubiquitinated form of USP8 was hardly detected under conditions of proteasome inhibition after

overexpression of WT USP8. However, the mutant USP8 (S718C) enhanced the amount of ubiquitinated USP8 (Fig. 4g), similarly to catalytically inactive USP8 (mutant USP8 C786S, Supplementary Fig. S3a), indicating that WT USP8 appeared to have an autodeubiquitination function and S718 of USP8 also might be an important site to conduct autodeubiquitination.

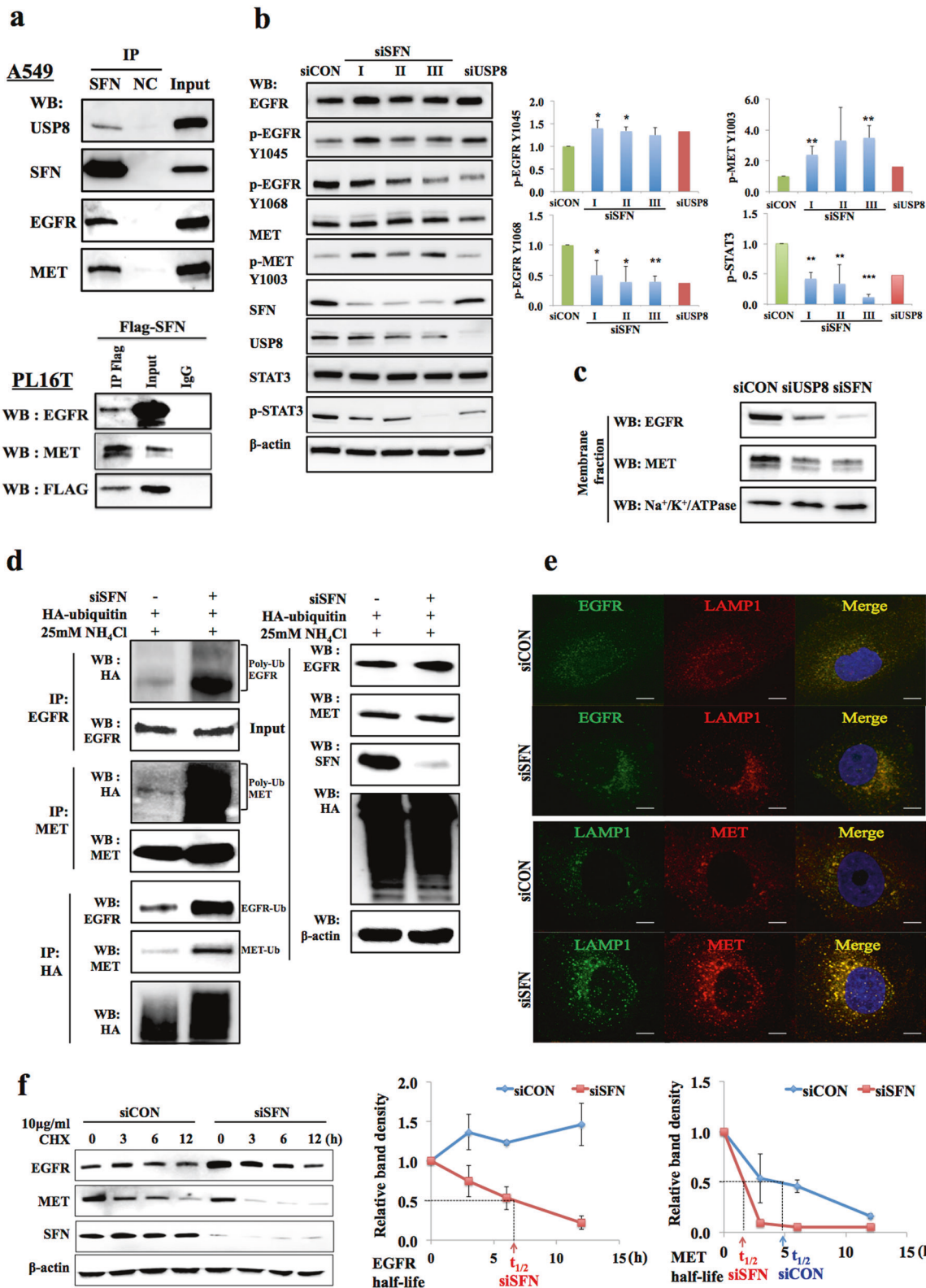
These results suggested that interaction of SFN with USP8 positively regulates autodeubiquitination activity to stabilize USP8 protein.

### SFN regulates the degradation pathway of RTKs in AIS cells

Previously, Huang et al. identified EGFR as a SFN binding partner in nasopharyngeal carcinoma using co-IP/MS analysis [29]. Even though we performed pull-down assay and LC-MS/MS analysis using two kinds of SFN plasmids, 3'-Flag-SFN and 5'-Flag-SFN with 4 times independent analysis, we did not find any interaction between SFN and RTKs such as EGFR and MET. We consider that our pull-down assay and LC-MS/MS analysis identified only proteins which directly interact with SFN, though previous co-IP/MS analysis might have also detected proteins which bind to SFN indirectly by forming protein complex. To confirm whether SFN binds to RTKs indirectly in lung adenocarcinoma cells, we performed co-IP and subsequent Western blotting. Expectedly, we found that SFN interacted with not only EGFR but also MET in A549 and PL16T cells (Fig. 5a).

To demonstrate whether SFN regulates the expression of EGFR and MET, similarly to USP8, which has been reported to regulate RTKs in advanced lung adenocarcinoma cells [30], we transfected PL16T cells with siRNA-SFN. Although knockdown of SFN did not alter total EGFR and MET (Fig. 5b), cell-surface proteins of EGFR and MET decreased similarly to knockdown of USP8 (Fig. 5c), indicating that SFN regulates cell-surface proteins of RTKs. Moreover, knockdown of SFN increased the expression of p-EGFR Y1045 and p-MET Y1003, which are associated with lysosomal degradation signaling (Fig. 5b). However, knockdown of SFN decreased the expression of p-EGFR Y1068, which is associated with cellular proliferation signaling, and p-STAT3, a downstream factor related to proliferation and apoptosis. Additionally, the tendency of RTKs down-regulation was consistent among three kinds of siRNA-SFN but each siRNA-SFN showed slightly different level of it, which might be due to differences of knockdown efficacy among siRNA sequences (Fig. 5b).

Next, a deubiquitination assay showed that expression of ubiquitinated EGFR and MET in the presence of NH<sub>4</sub>Cl, a lysosomal inhibitor, after knockdown of SFN was clearly higher than in the control (Fig. 5d), similarly to knockdown



of USP8 (Supplementary Fig. S3b). Moreover, IF with LAMP1, a lysosomal marker, showed that knockdown of SFN induced tight clusters distribution of lysosomal

vesicles possibly due to the accumulation of EGFR and MET (Fig. 5e), which budded from early endosome that may contain increased ubiquitinated EGFR and MET by

**Fig. 5** SFN regulates stabilization of RTKs in AIS cells. **a** To demonstrate interaction of endogenous USP8, EGFR, and MET with SFN, a lysate of A549 cells was immunoprecipitated with anti-SFN. As a negative control (NC), the cell lysate and protein A magnetic beads were incubated without antibody for 1 h at 4 °C. Since use of PL16T made it difficult to examine endogenous interaction of proteins, Co-IP using Flag antibody was performed after overexpression of Flag-SFN. The eluted IP sample was subjected to Western blotting using the indicated antibodies. **b** Expression of total and phosphorylated RTKs such as EGFR and MET and their downstream factor, STAT3, was assessed by Western blotting using PL16T cells transfected with siSFN. We performed three independent experiments and quantified each band size to show p-EGFR, p-MET, and p-STAT3 expression using a bar graph after normalization of each by total EGFR, MET, and STAT3, respectively. **c** Expression of membrane EGFR and MET was assessed using subcellular fractionation after transfection with siUSP8 or siSFN. The extracted membrane proteins (30 µg) were heated by 37 °C for 30 min and used for electrophoresis on 7.5% Mini-PROTEAN TGX Precast Gels. Na+/K+/ATPase were used for plasma membrane marker. **d** Expression of ubiquitinated EGFR and MET was examined by co-IP after transfection with siSFN accompanied by overexpression of HA-ubiquitin in PL16T. The cells were treated with 25 mM NH<sub>4</sub>Cl (a lysosomal inhibitor) for 4 h, leading to accumulation of ubiquitinated EGFR or MET at the lysosome. **e** After siSFN transfection, ubiquitinated EGFR and MET, which were destined for lysosomal degradation, were assessed by IF after staining for LAMP1 (a lysosomal marker) in PL16T. EGFR and MET were immunostained with respective antibodies, and their accumulation at lysosomes after treatment with 25 mM NH<sub>4</sub>Cl (a lysosomal inhibitor) for 4 h was examined. Scale bar, 10 µm. **f** The half-life of EGFR and MET was assessed by Western blotting after transfection with siSFN in PL16T. The cells were treated with cycloheximide (CHX; a protein synthesis inhibitor) for the indicated time. β-actin was used as a control to verify equal loading of protein (20 µg).

inhibiting recycling pathway, similarly to knockdown of USP8 (Supplementary Fig. S3c). Thus, the half-life of EGFR and MET after knockdown of SFN was shorter than in the siCON treated with cycloheximide, a protein synthesis inhibitor (Fig. 5f).

Taken together, these results suggested that SFN prevents the lysosomal degradation of RTKs via USP8 to enhance the recycling of RTKs back to the plasma membrane.

### Impairment of USP8 and SFN interaction negatively regulates RTKs in AIS cells

According to previous studies [9, 31], SFN has four important residues, Lys49, Arg56, Arg129, and Tyr130, for recognition of phosphoserine on target proteins. We generated three SFN mutants, K49A, R56A, and R129A/Y130A, and performed co-IP using A549 cells to confirm whether these sites are related to binding with USP8. We found that the SFN mutants abolished interaction with endogenous USP8 almost completely (Fig. 6a). Additionally, we generated multiple SFN mutants containing the four point mutations. Since PL16T cells have low

expression of USP8 and SFN, we overexpressed WT USP8 and either WT or multiple SFN mutants to examine their interaction with USP8. Consistent with the single point mutant form of SFN, the multiple mutant forms also abolished not only USP8 but also EGFR and MET interaction (Fig. 6b). This suggested that impairment of the SFN-USP8 complex might downregulate RTKs expression by inhibiting the interaction of RTKs with the SFN-USP8 complex.

Next, to clarify whether SFN interaction with USP8 regulates the expression of RTKs and their downstream factor, we transfected PL16T cells individually with the WT USP8 or the mutant USP8 (S718C) and examined the resulting impairment of SFN interaction. As expected, the mutant USP8 (S718C) reduced the expression of RTKs, EGFR and MET, as well as a downstream factor, p-STAT3, in comparison to the expression after transfection with WT USP8 (Fig. 6c). Moreover, cotransfection with the mutant USP8 and SFN reduced the expression of both EGFR and MET, as well as that of p-STAT3, in comparison to the expression after cotransfection with WT USP8 and SFN (Fig. 6d), indicating that these residues of USP8 and SFN are responsible for recognition and formation of a complex to regulate the expression of RTKs.

Collectively, these findings suggested that binding of SFN with USP8 is essential for stabilization of RTKs through deubiquitination.

### SFN interaction with USP8 is regulated by PP1 in lung adenocarcinoma cells

The 14-3-3 BM of USP8 (RSYSSP) is essential for USP8 to interact with the 14-3-3 members, and S718 of the 14-3-3 binding motif in USP8 is a critical biological phosphorylation site [32]. On the basis of our results, we speculated that phosphorylation of USP8 at 14-3-3 BM is crucial for SFN binding and regulation of RTKs (Figs. 4f, 6c). Panner et al. have reported that the enzymatic activity of USP8 is dependent on AKT, a serine/threonine-specific protein kinase [33]. To clarify the involvement of AKT in regulation of USP8 phosphorylation on its 14-3-3 BM, we examined the endogenous interaction of USP8 and pAKT and then treated A549 cells with the PI3K-AKT pathway inhibitor, LY294002. Treatment with LY294002 apparently decreased the USP8 phosphorylation on 14-3-3 BM and also impaired the binding of USP8 with SFN (Supplementary Figs. S4a and S4b). Consistently, treatment with LY294002 increased ubiquitinated EGFR and MET (Supplementary Fig. S4c). However, treatment with LY294002 did not alter ubiquitinated EGFR and MET when mutant USP8 (S718C) was transfected (Supplementary Fig. S4d), because mutant USP8 impaired binding with SFN independently of PI3K-AKT pathway inhibitor. These facts indicate that AKT is a positive regulator for USP8 and SFN

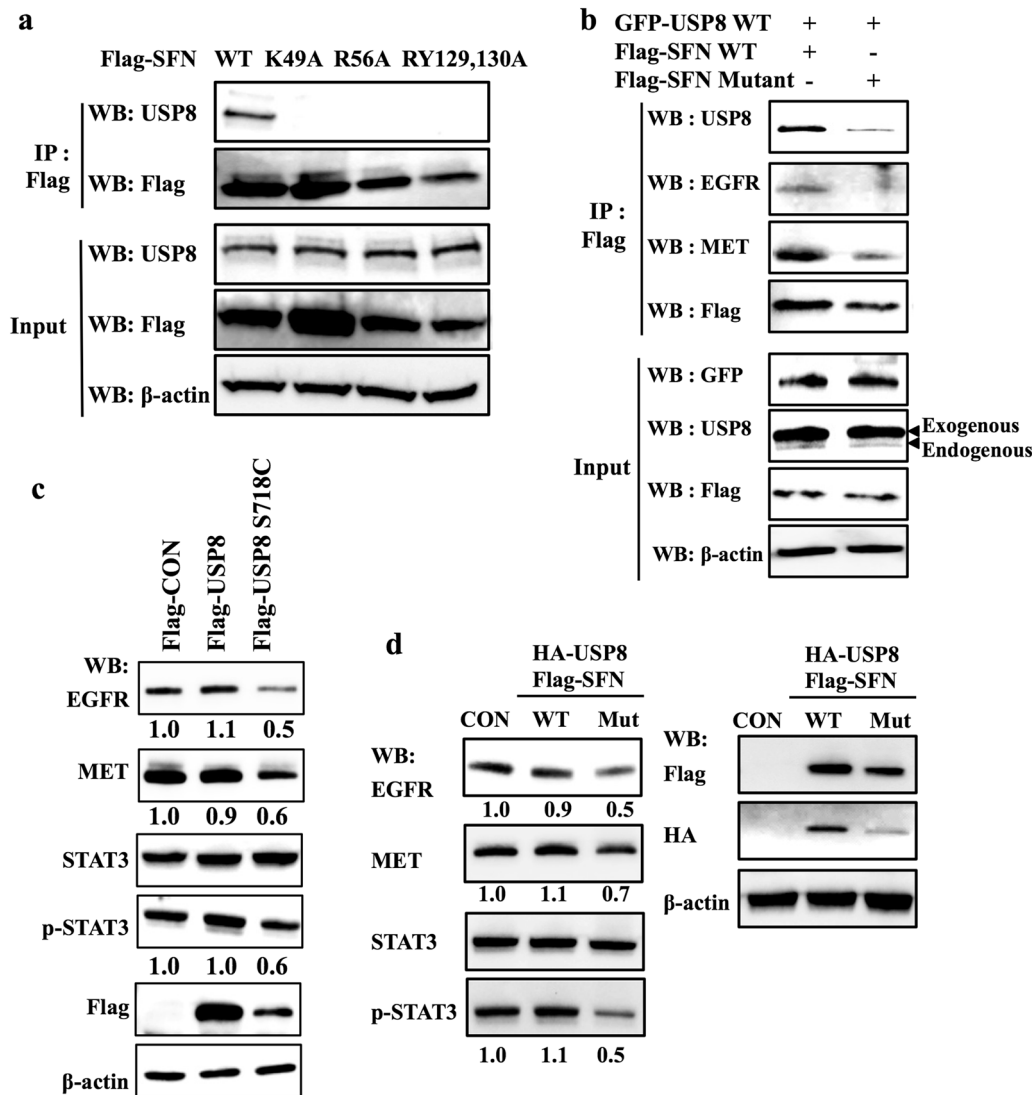


**Fig. 6** USP8-SFN complex regulates RTKs and downstream signaling in AIS cells. **a** We generated three types of SFN mutant containing one or two point mutations at residues 49, 56, and both 129 and 130. Cells transfected with each point mutant SFN were subjected to co-IP to analyze their interaction with USP8 in A549. **b** Mutant SFN contained four multiple point mutations at residues 49, 56, 129, and 130, which are the important residues for recognition of phospho-target proteins such as phospho-USP8. Cells transfected with SFN wild-type (WT) or SFN mutant accompanied by USP8 WT were tested for their

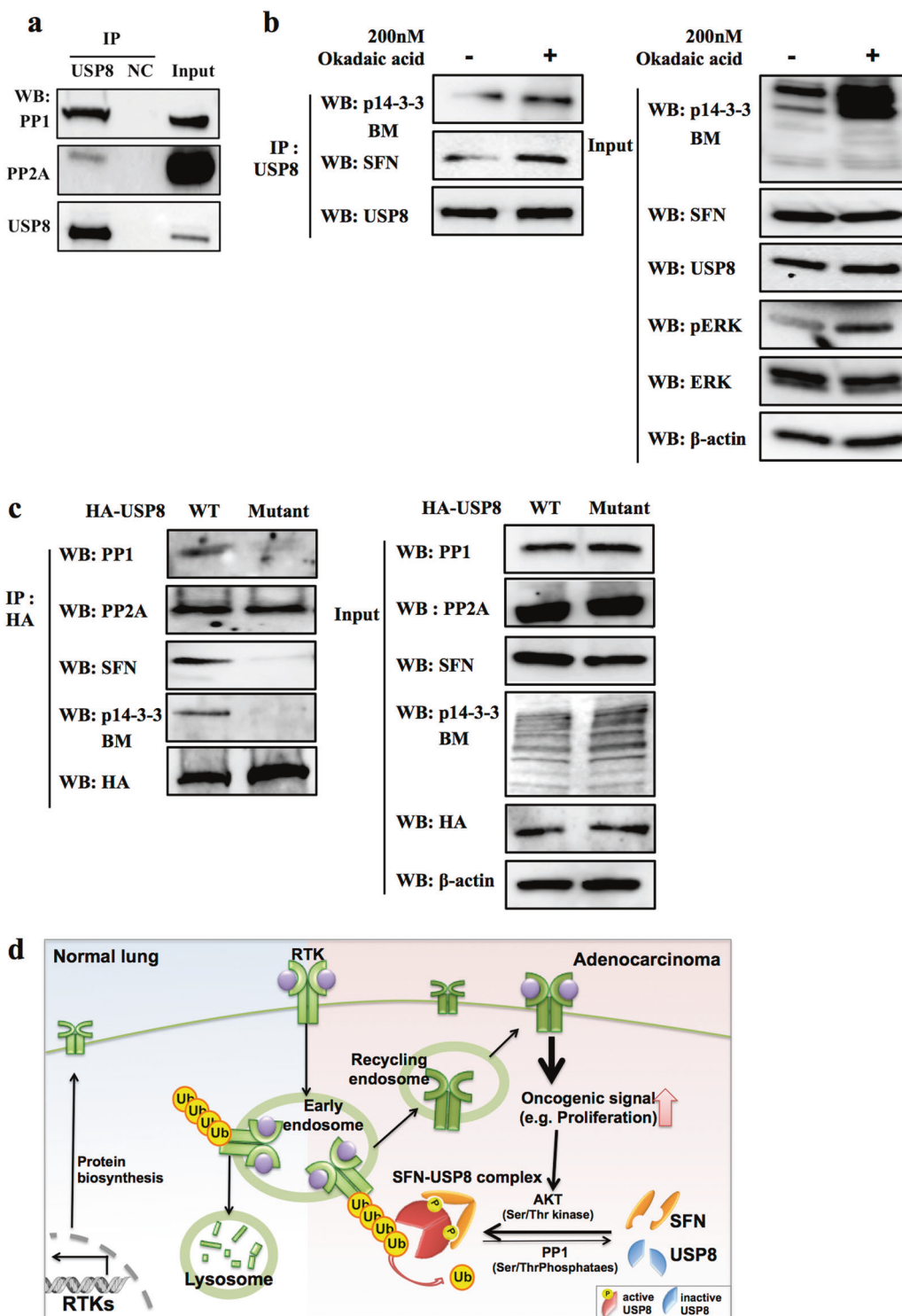
interaction with USP8 by co-IP in PL16T. **c** After transfection with the Flag-USP8 WT or mutant (S718C), expression of RTKs and downstream factors was assessed by Western blotting in PL16T. **d** After cotransfection with both WT or mutant HA-USP8 and Flag-SFN, expression of RTKs and downstream factors was assessed by Western blotting in PL16T. The mutant USP8 contained S718C and the mutant SFN harbored K49A, R56A, R129Y, and Y130A.  $\beta$ -actin was used as a control to verify equal loading of protein (20  $\mu$ g)

interaction and their activity in RTKs stabilization. However, the specific phosphatase responsible for reverse USP8 phosphorylation from the active to the inactive form remained unknown.

Since PP1 and PP2A are important regulators of 14-3-3 binding to its target protein [10], we examined endogenous interaction between USP8 and PP1 or PP2A by co-IP in A549 cells. As expected, we found that endogenous PP1 and PP2A each interacted with USP8 (Fig. 7a) and that treatment of cells with a specific PP1/PP2A inhibitor, okadaic acid (OA), led to a marked increase in USP8

phosphorylation on 14-3-3 BM and binding of USP8 to SFN (Fig. 7b). Consistently, OA diminished ubiquitination of EGFR and MET but mutant USP8 (S718C) was not affected by OA because mutant USP8 does not have phosphorylation site, unlike WT USP8 (Supplementary Figs. S5a and S5b). These results indicated that inhibition of PP1 or PP2A enhances USP8 and SFN interaction and USP8 activity in RTKs stabilization in lung adenocarcinoma cells.

Next, to demonstrate whether PP1 or PP2A modulates USP8 dephosphorylation at 14-3-3 BM, we confirmed their



interaction by performing co-IP under conditions of WT or mutant USP8 (S718C) overexpression. We found that impairment of the serine-phosphorylation of mutant USP8, rendering it unable to bind with SFN, abolished PP1 binding but not PP2A binding (Fig. 7c). On the basis of this result, we speculated that PP1 and SFN might competitively

interact with USP8 at S718 of 14-3-3BM to regulate USP8 deubiquitinase activity, unlike PP2A. As expected, mutant SFN induced interaction of PP1 with USP8, when compared with WT SFN (Supplementary Fig. S5c). Taken together, the present results suggested that PP1 contributes to the regulation of 14-3-3 BM phosphorylation in

**Fig. 7** PP1 regulates the USP8-SFN complex by dephosphorylation of the 14-3-3 binding motif. **a** To demonstrate the interaction of endogenous PP1 and PP2A with USP8, a lysate of A549 cells was immunoprecipitated with anti-USP8. As a negative control (NC), the cell lysate and protein A magnetic beads were incubated without antibody for 1 h at 4 °C. The eluted IP sample was subjected to Western blotting using the indicated antibodies. **b** The SFN-USP8 complex was evaluated by co-IP and Western blotting. p14-3-3 BM is the phospho14-3-3 binding motif, indicating phospho-USP8 which facilitates binding to SFN. A549 cells were treated with 200 nM okadaic acid, a PP1/PP2A (serine/threonine phosphatase) specific inhibitor, for 1 h. pERK was used as a positive control for the serine/threonine phosphatase inhibitor. **c** To assess whether PP1 or PP2A utilizes p14-3-3 BM for binding with USP8, WT (wild-type) or mutant (S718C) HA-USP8 was transfected into A549 cells, and 24 h after transfection a lysate of the cells was subjected to co-IP with anti-HA. The eluted IP sample was subjected to Western blotting using the indicated antibodies. β-actin was used as a control to verify equal loading of protein (20 µg). **d** A model of the pathway for regulation of RTKs by the SFN-USP8 complex in normal lung and adenoacrinoma cells. Ligand-bound RTKs are internalized through endocytosis and form early endosomes. Some internalized RTKs are subjected to lysosomal degradation, but others undergo recycling back to the plasma membrane via recycling endosomes through USP8 deubiquitinating activation. In normal cells, ubiquitinated RTKs strictly maintain the balance between the recycling and degradation pathways, as well as physiological regulation of biosynthesis. However, in tumor cells, SFN and USP8 show abnormal overexpression and their complex facilitates recycling of RTKs to the plasma membrane through deubiquitination of ubiquitinated RTKs. Moreover, interaction of USP8 and SFN is regulated through phosphorylation by AKT or PP1. Hyperactivation of AKT in tumor cells accelerates the binding of phospho-USP8 to SFN, and SFN also induces stabilization of phospho-USP8 by protecting it from dephosphorylation via PP1. Subsequently, the SFN and USP8 complex protects RTKs from degradation and contributes to aberrant cellular proliferation

USP8, having a negative feedback effect on USP8 activity (Fig. 7d).

## Discussion

Previous studies have indicated that each of the 14-3-3 proteins has unique functions, which are context-dependent and also organ-dependent or tissue-dependent [6]. SFN in particular is evolutionarily distinct from all of the other 14-3-3 proteins from the viewpoint of sequence conservation [34] and shows the closest association with lung cancer [5]. In this regard, abnormal regulation of USP8 induced by SFN is a unique and tissue-selective phenomenon in lung adenocarcinoma (Fig. 1). Here, we found that SFN and USP8 facilitate cellular proliferation and inhibit apoptosis, and these phenomena were induced most markedly in the PL16T cell line, which was established from AIS, an early-stage form of adenocarcinoma, in comparison with the other cell lines derived from advanced adenocarcinomas (Fig. 3). Previously, we had found that DNA demethylation-triggered abnormal overexpression of SFN is an early

event in the malignant progression of lung adenocarcinoma [4, 35]. We also reported that similarly to SFN, overexpression of USP8 is an oncogenic alteration at the early stage [20]. Although the level of SFN expression is associated with patient outcome, that of USP8 is not (Fig. 2). Therefore, the biological effect of USP8 might be included in that of the multifunctional protein, SFN, and the expression of USP8 itself may not influence the final patient outcome.

Additionally, our results indicated that USP8 and SFN may have an important effect in maintaining their mutual stability (Fig. 4). Recently, Kim et al. demonstrated that among 14-3-3 proteins, 14-3-3 $\gamma$  is specifically regulated by and interacts with USP37, inhibiting its degradation by Lys-48 and Lys-63 branched polyubiquitination in lung, breast, ovarian, and colorectal cancer cells [36]. That report suggested that each of the 14-3-3 proteins might have specific regulatory and binding DUB partners to enhance their stability.

Post-translational modification including ubiquitination by ubiquitin ligases and deubiquitination by the DUBs is a key mechanism to regulate protein stability such as cell-surface receptors [37]. Recent studies have screened DUBs involved in regulation of EGFR degradation including AMSH, USP8, USP9X, which regulated EGFR initial endocytosis by stabilization of Esp15 [38], and Cezanne-1, which was frequently amplified and promoting tumor aggressiveness in breast cancers [39], using siRNA library of the majority of human DUBs. Among them, Clague et al. has reported that AMSH and USP8 are required to interact with Hrs-STAM endosomal sorting complex at early endosome, regulating STAM stability [40, 41]. However, Komada et al. showed that USP8 is recruited by Hrs-STAM and directly binds with ubiquitinated EGFR to deubiquitinate it [42]. These different findings imply a complicated mechanism underlying receptor protein degradation. On the basis of these reports, multiple processes achieve the efficient control on trafficking of ubiquitinated receptor proteins to lysosomal degradation. However, controlling mechanism of RTKs trafficking to lysosome in particular cancer cells has not been clarified yet.

In the present study, we confirmed that USP8 binds to and regulates EGFR and MET to accelerate their deubiquitination (Fig. 5 and Supplementary Fig. S3). Similarly to USP8, SFN was also shown to be a binding partner of EGFR and MET (Fig. 5a), and knockdown of SFN strongly induced the degradation signaling of EGFR and MET mediated with phosphorylation at Y1045 and Y1003, respectively (Fig. 5b). Consequentially, knockdown of SFN decreased cell-surface EGFR and MET (Fig. 5c) and cellular proliferation signaling (Fig. 5b). Activation of RTKs by binding ligands leads to autophosphorylation of receptor catalytic domain, for example pY1068 of EGFR, and serve

as docking sites for activation of downstream signal cascade. On the other hand, RTKs activity is negatively controlled by protein tyrosine phosphatases (PTPs) leading to inhibition of RTK autophosphorylation or by ubiquitin ligase Cbl through binding with pY1045 of EGFR and pY1003 of MET for lysosomal degradation [43]. Moreover, previous report found that degree of phosphorylation at each site could be different among Y992, Y1045, Y1068, Y1086, Y1148, and Y1173 depending on concentration of EGF or TGF-alpha [44]. Consistent with this report, we found that knockdown of SFN showed different level of pY1045 and pY1068 of EGFR, suggesting that SFN might play role as a positive regulator for activation of RTKs.

Additionally, our finding that lack of SFN binding with USP8 induced ubiquitination and reduced the half-life of RTKs supports the possibility that SFN promotes activity and stability of USP8 associated with RTK stabilization in lung adenocarcinoma (Figs 5 and 6). Unlike SFN, 14-3-3 epsilon and beta, which are highly expressed in mammalian brain [6], inhibit USP8 activity in Cushing's disease [21, 22, 45] and mouse T-cells [24] by blocking the post-translational modification, cleavage of USP8 which is leading to hyperactive deubiquitination of EGFR. Moreover, mutations of USP8 in Cushing's disease frequently occur at the 14-3-3 binding motif, leading to upregulation of EGFR and subsequent hyperproduction of ACTH, the hallmark of Cushing's disease [32]. In contrast to the findings for Cushing's disease, our findings did not show any somatic mutation at the 14-3-3 binding motif of USP8 in lung adenocarcinoma tissue nor any fragmentary form of USP8 in lung adenocarcinoma cells (Supplementary Fig. S6).

USP8 enzymatic activity is dependent on phosphorylation by c-Src, a non-receptor tyrosine kinase [46], and AKT, a serine/threonine-specific protein kinase [33]. On the other hand, no phosphatase specific for USP8 has yet been identified. Here, we found that USP8 interacted with PP1, a serine/threonine phosphatase, similarly to a previous report showing that PP1 negatively regulates 14-3-3 binding to target proteins such as Cdc25C [10]. Moreover, our results showed that PP1 binds to USP8 at 14-3-3 BM, similarly to SFN, and thus SFN and PP1 might competitively bind with USP8 (Fig. 7). Therefore, we speculate that SFN might have higher binding affinity for USP8 than for PP1, or that overexpression of SFN might promote interaction with USP8 and induce a conformational change in USP8 that increases its enzymatic activity and stability in lung adenocarcinoma (Fig. 7d).

Many molecularly targeted drugs have been developed for advanced lung adenocarcinomas harboring EGFR mutations or ALK rearrangement [47, 48]. Although TKIs for EGFR and EML4-ALK are initially very effective, most tumors subsequently acquire resistance to the drugs. Byun

et al. reported that a USP8 inhibitor suppressed both growth and tumor formation of both TKI-resistant and -sensitive NSCLC cells by inducing degradation of RTKs, and suggested that USP8 might be a preferable therapeutic target for overcoming acquired resistance [30]. However, it would be easily envisaged that USP8 inhibitor might dysregulate the physiologically important functions of USP8 in normal tissues, causing severe adverse effects. In support of this, USP8 was first demonstrated as a growth-regulated ubiquitin isopeptidase [49], deletion of which caused embryonic lethality in mice [18]. On the other hand, SFN shows high tumor-specific expression and induces aberrant USP8 activation in lung adenocarcinoma. Therefore, we believe that an SFN inhibitor would be a more selective and desirable therapeutic target for lung adenocarcinoma than USP8, offering the possibility of effectiveness against TKI-resistant tumors.

In summary, we have revealed that SFN preserves aberrant regulation of USP8 and subsequently protects RTKs from lysosomal degradation, resulting in hyperactivation of these signaling pathways. SFN may be central to the development of a useful therapeutic strategy for both early and advanced lung adenocarcinomas.

## Materials and methods

### Cell lines and culture conditions

The PL16T cell line was established in our laboratory from a surgically resected AIS of the lung [27]. PL16T cells were maintained in MCDB153HAA (Wako, Osaka, Japan) supplemented with 2% FBS (Sigma-Aldrich, St. Louis, MO), 0.5 ng/ml human-EGF (Toyobo, Tokyo, Japan), 5 µg/ml human-insulin (Wako), 72 ng/ml hydrocortisone (Wako), 40 µg/ml human-transferrin (Sigma-Aldrich), and 20 ng/ml sodium selenate (Sigma-Aldrich). PC9 cells and A549 cells were maintained as described previously [50]. The cells were cultured in a 5% CO<sub>2</sub> incubator at 37 °C and passaged every 3–4 days.

### Transfection with small interfering RNA (siRNA)/expression vectors

USP8-specific or SFN-specific siRNAs from Thermo Fisher Scientific and a nucleic acid transfer agent, lipofectamine RNAiMAX (Thermo Fisher Scientific), were used for siRNA transfection as described previously [4] and detailed in the Supplementary Information. Plasmid DNA was purified using an EndoFree Plasmid Maxi kit (QIAGEN, Hilden, Germany). Fugene HD (Promega, Madison, WI) was used for plasmid transfection in accordance with the manufacturer's protocol.

## DNA constructs and point mutagenesis

Expression vectors for full-length wild-type human Flag-HA-USP8 and HA-14-3-3 epsilon/Myc-14-3-3 zeta were purchased from Addgene (Cambridge, MA). Construction of Flag-SFN and pSFN (siSFN-resistant) has been described previously [4]. HA-ubiquitin and wild-type GFP-USP8 were obtained from Professor Yasunori Kanaho (University of Tsukuba, Japan). Mutagenesis to create constructs encoding the mutant form of Flag-HA-USP8 and Flag-SFN was carried out with the PrimeSTAR Mutagenesis Basal kit (Takara, Shiga, Japan) in accordance with the manufacturer's protocol, as detailed in the Supplementary Information. Sequences of all constructs were verified by Sanger sequencing.

## Patients and sample selection

We selected 193 specimens of lung adenocarcinomas that had been surgically resected at the University of Tsukuba Hospital (Ibaraki, Japan) between 1999 and 2007. Follow-up information for all of the corresponding patients was obtainable from the medical records. Informed consent for use of their materials had been obtained from all of the patients. The study was approved by the institutional ethics review committee and the lung adenocarcinoma cases were classified according to the UICC TNM classification of malignant tumors (seventh edition) and the World Health Organization (WHO) classification of malignant tumors (fourth edition) [51, 52].

## Immunohistochemistry

We used 4-μm-thick tissue sections from formalin-fixed paraffin-embedded (FFPE) tissue microarray (TMA) blocks. Each TMA block comprised 24 specimens containing lung adenocarcinoma tissue in a 48-core slide. Immunostaining has been described previously [20]. We scored SFN and USP8 according to the intensity of cytoplasmic staining. The staining was judged to be positive when the cytoplasm of the tumor cells was stained more strongly than that of the alveolar epithelium. Testis tissue was used as a positive control for USP8 and lung adenocarcinoma tissue with high SFN expression, which we had used in a previous study [4], was used for SFN. Anti-USP8 polyclonal rabbit antibody (Bethyl Laboratories, Montgomery, TX) and anti-SFN monoclonal mouse antibody (Sigma-Aldrich) were used as the primary antibodies.

## Cellular proliferation assay

Cells were seeded in six-well plates after siRNA transfection and cultured for the indicated time periods. The

adherent cells were collected and suspended in 0.4% trypan blue solution (Thermo Fisher Scientific). The number of cells was counted using a hemacytometer. Three replicates were prepared for each group. For analysis of cellular proliferation activity, a WST-1 kit (Roche Diagnostic, Mannheim, Germany) was used in accordance with the manufacturer's protocol after siRNA transfection.

## Apoptosis assay

After siRNA transfection for 48 h, both adherent and floating cells were collected and extracted proteins using Mammalian Protein Extraction Reagent (M-PER; Thermo Fisher Scientific) containing a Halt protease and phosphatase inhibitor cocktail (Thermo Fisher Scientific). The positive control for apoptosis was a lysate of PL16T or A549 treated with 10 μM camptothecin (Sigma-Aldrich) for 24 h. For evaluation of apoptosis, we performed Western blotting to detect cleaved caspase 3.

## Western blotting

Total proteins were prepared on ice using M-PER for cultured cells or Tissue Protein Extraction Reagent (T-PER; Thermo Fisher Scientific) for fresh tissue containing a Halt protease and phosphatase inhibitor cocktail. The total protein in the lysates was measured using a BCA protein assay kit (Thermo Fisher Scientific). Total proteins (20 μg) were used for electrophoresis on 7.5%, 10%, or 12% Mini-PROTEAN TGX Precast Gels (Bio-Rad Laboratories, Hercules, CA) and transferred as described previously [20]. The blots were then blocked and probed with various antibodies as detailed in the Supplementary Information and finally detected by the chemiluminescence method using SuperSignal West Femto Maximum sensitivity substrate (Thermo Fisher Scientific).

## Coimmunoprecipitation (Co-IP)

The cells were transfected with appropriate plasmids for 24 h. After transfection, the total protein was extracted using IP Lysis Buffer (Thermo Fisher Scientific) containing a Halt protease and phosphatase inhibitor cocktail (Thermo Fisher Scientific). The cell extracts were concentrated using Amicon Ultra 3k (Merck Millipore, Billerica, MA) by centrifugal filtration, supplemented with an appropriate antibody and washed with protein A or G magnetic beads (Bio-Rad Laboratories), and incubated at 4 °C overnight. The beads were subsequently pelleted on a magnetic separation rack for 15 s and washed 3 times using IP Lysis Buffer. The samples were then boiled at 95 °C for 5 min to elute the immunocomplexed proteins. Levels of proteins in

the elution products were assessed by Western blotting using the appropriate antibodies.

### Immunofluorescence (IF)

After siRNA transfection, the cells were plated on collagen-coated cover slides (Iwaki Biosciences, Tokyo, Japan) and fixed with 10% neutral buffered formalin and were incubated with primary antibodies for 1 h, as detailed in the Supplementary Information. They were then incubated with anti-mouse IgG conjugated Alexa Fluor 488 secondary antibody and anti-rabbit IgG conjugated Alexa Fluor 568 secondary antibody (1:1000, Thermo Fisher Scientific) for 1 h. Coverslips were mounted onto glass slides with mounting medium (Fluoromount-G, SouthernBiotech, AL, USA) after nuclear staining with DAPI (1:5000, Sigma-Aldrich) for 5 min. The cells were analyzed using a confocal laser scanning microscope (LSM700; Carl Zeiss, Oberkochen, Germany) using a Plan-Apochromat 63 $\times$ /1.40 Oil DIC M27 objective. The following setting were used: Filters were used: Track 1 Ch2, 420–1000; Track2 Ch1, BP 420–475 + BP 500–610; and Track3 Ch2, 568–1000. Beam splitters were used MBS 405/488/555/639 and DBS1 420 nm for Track1, 576 nm for Track2, and 568 nm for Track3. Images were taken using lasers of 405 nm (Track1) for DAPI stain, 488 nm (Track2) for Alexa Fluor 488 stain, and 555 nm (Track3) for Alexa Fluor 568 stain.

### Deubiquitination assay for detecting ubiquitinated proteins

The cells were transfected with siRNA for 24 h followed by HA-ubiquitin for 24 h. After transfection, the cells were treated with 25 mM NH<sub>4</sub>Cl (Sigma-Aldrich), a lysosomal inhibitor, for 4 h or 10  $\mu$ M MG132 (Sigma-Aldrich), a proteasome inhibitor, for 16 h at 37 °C in a 5% CO<sub>2</sub> incubator. The total protein was extracted using IP Lysis Buffer (Thermo Fisher Scientific) containing a Halt protease and phosphatase inhibitor cocktail (Thermo Fisher Scientific) and 10 mM N-ethylmaleimide (NEM; Sigma-Aldrich), a deubiquitinase inhibitor. Ubiquitinated proteins in the lysate were assessed by co-IP and Western blotting using the appropriate antibodies.

### Statistical analysis

Group results are expressed as mean  $\pm$  SD. Data were compared between groups using the *t* test to calculate 2-tailed distributions and a paired *t* test. SPSS 22 statistical software (SPSS, Chicago, IL) was used for IHC data analysis as follows. Correlations of clinicopathological features with USP8 or SFN expression were analyzed using the chi-

squared test. Disease-free survival according to USP8 or SFN expression was examined using the Kaplan-Meier method, and the significance of differences between survival curves was evaluated using the log-rank test.

**Acknowledgements** We express our appreciation to Professor Yasu-nori Kanaho and Dr. Yuji Funakoshi for research support and kindly providing the plasmids and reagents. We also thank Professor Mitsuyasu Kato and Dr. Hiroyuki Suzuki (Faculty of Medicine, University of Tsukuba) for research support and Professor Flaminia Miyamasu (Medical English Communications Center, University of Tsukuba) for critical review of this manuscript.

### Compliance with ethical standards

**Conflict of interest** The authors declare that they have no conflict of interest.

### References

1. Siegel RL, Miller KD, Jemal A. Cancer statistics, 2016. CA Cancer J Clin. 2016;66:7–30.
2. Noguchi M, Morikawa A, Kawasaki M, Matsuno Y, Yamada T, Hirohashi S, et al. Small adenocarcinoma of the lung. Histologic characteristics and prognosis. Cancer. 1995;75:2844–52.
3. Kakinuma R, Noguchi M, Ashizawa K, Kuriyama K, Maeshima AM, Koizumi N, et al. Natural history of pulmonary subsolid nodules: a prospective multicenter study. J Thorac Oncol. 2016;11:1012–28.
4. Shiba-Ishii A, Kano J, Morishita Y, Sato Y, Minami Y, Noguchi M. High expression of stratifin is a universal abnormality during the course of malignant progression of early-stage lung adenocarcinoma. Int J Cancer. 2011;129:2445–53.
5. Shiba-Ishii A, Kim Y, Shiozawa T, Iyama S, Satomi K, Kano J, et al. Stratifin accelerates progression of lung adenocarcinoma at an early stage. Mol Cancer. 2015;14:142.
6. Aghazadeh Y, Papadopoulos V. The role of the 14-3-3 protein family in health, disease, and drug development. Drug Discov Today. 2016;21:278–87.
7. Yaffe MB, Rittinger K, Volinia S, Caron PR, Aitken A, Leffers H, et al. The structural basis for 14-3-3:phosphopeptide binding specificity. Cell. 1997;91:961–71.
8. Hermeking H. The 14-3-3 cancer connection. Nat Rev Cancer. 2003;3:931–43.
9. Smith AJ, Daut J, Schwappach B. Membrane proteins as 14-3-3 clients in functional regulation and intracellular transport. Physiology. 2011;26:181–91.
10. Dougherty MK, Morrison DK. Unlocking the code of 14-3-3. J Cell Sci. 2004;117:1875–84.
11. Fraile JM, Quesada V, Rodriguez D, Freije JM, Lopez-Otin C. Deubiquitinases in cancer: new functions and therapeutic options. Oncogene. 2012;31:2373–88.
12. Xia R, Jia H, Fan J, Liu Y, Jia J. USP8 promotes smoothened signaling by preventing its ubiquitination and changing its subcellular localization. PLoS Biol. 2012;10:e1001238.
13. Mukai A, Yamamoto-Hino M, Awano W, Watanabe W, Komada M, Goto S. Balanced ubiquitylation and deubiquitylation of Frizzled regulate cellular responsiveness to Wg/Wnt. EMBO J. 2010;29:2114–25.
14. Wu X, Yen L, Irwin L, Sweeney C, Carraway KL 3rd. Stabilization of the E3 ubiquitin ligase Nrdp1 by the deubiquitinase enzyme USP8. Mol Cell Biol. 2004;24:7748–57.

15. Mizuno E, Iura T, Mukai A, Yoshimori T, Kitamura N, Komada M. Regulation of epidermal growth factor receptor downregulation by UBPY-mediated deubiquitination at endosomes. *Mol Biol Cell*. 2005;16:5163–74.
16. Meijer IM, van Leeuwen JE. ERBB2 is a target for USP8-mediated deubiquitination. *Cell Signal*. 2011;23:458–67.
17. Smith GA, Fearnley GW, Abdul-Zani I, Wheatcroft SB, Tomlinson DC, Harrison MA, et al. VEGFR2 trafficking, signaling and proteolysis is regulated by the ubiquitin isopeptidase USP8. *Traffic*. 2016;17:53–65.
18. Niendorf S, Oksche A, Kissner A, Lohler J, Prinz M, Schorle H, et al. Essential role of ubiquitin-specific protease 8 for receptor tyrosine kinase stability and endocytic trafficking in vivo. *Mol Cell Biol*. 2007;27:5029–39.
19. Takeuchi K, Ito F. Receptor tyrosine kinases and targeted cancer therapeutics. *Biol Pharm Bull*. 2011;34:1774–80.
20. Kim Y, Shiba-Ishii A, Nakagawa T, Husni RE, Sakashita S, Takeuchi T, et al. Ubiquitin-specific protease 8 is a novel prognostic marker in early-stage lung adenocarcinoma. *Pathol Int*. 2017;67:292–301.
21. Reincke M, Sbiera S, Hayakawa A, Theodoropoulou M, Osswald A, Beuschlein F, et al. Mutations in the deubiquitinase gene USP8 cause Cushing's disease. *Nat Genet*. 2015;47:31–8.
22. Ma ZY, Song ZJ, Chen JH, Wang YF, Li SQ, Zhou LF, et al. Recurrent gain-of-function USP8 mutations in Cushing's disease. *Cell Res*. 2015;25:306–17.
23. Ballif BA, Cao Z, Schwartz D, Carraway KL 3rd, Gygi SP. Identification of 14-3-3epsilon substrates from embryonic murine brain. *J Proteome Res*. 2006;5:2372–9.
24. Dufner A, Kissner A, Niendorf S, Basters A, Reissig S, Schonle A, et al. The ubiquitin-specific protease USP8 is critical for the development and homeostasis of T cells. *Nat Immunol*. 2015;16:950–60.
25. Mizuno E, Kitamura N, Komada M. 14-3-3-dependent inhibition of the deubiquitinating activity of UBPY and its cancellation in the M phase. *Exp Cell Res*. 2007;313:3624–34.
26. Benzinger A, Muster N, Koch HB, Yates JR 3rd, Hermeking H. Targeted proteomic analysis of 14-3-3 sigma, a p53 effector commonly silenced in cancer. *Mol Cell Proteom*. 2005;4:785–95.
27. Shimada A, Kano J, Ishiyama T, Okubo C, Iijima T, Morishita Y, et al. Establishment of an immortalized cell line from a pre-cancerous lesion of lung adenocarcinoma, and genes highly expressed in the early stages of lung adenocarcinoma development. *Cancer Sci*. 2005;96:668–75.
28. Mei Y, Hahn AA, Hu S, Yang X. The USP19 deubiquitinase regulates the stability of c-IAP1 and c-IAP2. *J Biol Chem*. 2011;286:35380–7.
29. Huang WG, Cheng AL, Chen ZC, Peng F, Zhang PF, Li MY, et al. Targeted proteomic analysis of 14-3-3sigma in nasopharyngeal carcinoma. *Int J Biochem Cell Biol*. 2010;42:137–47.
30. Byun S, Lee SY, Lee J, Jeong CH, Farrand L, Lim S, et al. USP8 is a novel target for overcoming gefitinib resistance in lung cancer. *Clin Cancer Res*. 2013;19:3894–904.
31. Li Z, Liu JY, Zhang JT. 14-3-3sigma: the double-edged sword of human cancers. *Am J Transl Res*. 2009;1:326–40.
32. Sbiera S, Deutschbein T, Weigand I, Reincke M, Fassnacht M, Allolio B. The new molecular landscape of Cushing's disease. *Trends Endocrinol Metab*. 2015;26:573–83.
33. Panner A, Crane CA, Weng C, Feletti A, Fang S, Parsa AT, et al. Ubiquitin-specific protease 8 links the PTEN-Akt-AIP4 pathway to the control of FLIPS stability and TRAIL sensitivity in glioblastoma multiforme. *Cancer Res*. 2010;70:5046–53.
34. Wilker EW, Grant RA, Artim SC, Yaffe MB. A structural basis for 14-3-3sigma functional specificity. *J Biol Chem*. 2005;280:18891–8.
35. Shiba-Ishii A, Noguchi M. Aberrant stratifin overexpression is regulated by tumor-associated CpG demethylation in lung adenocarcinoma. *Am J Pathol*. 2012;180:1653–62.
36. Kim JO, Kim SR, Lim KH, Kim JH, Ajjappala B, Lee HJ, et al. Deubiquitinating enzyme USP37 regulating oncogenic function of 14-3-3gamma. *Oncotarget*. 2015;6:36551–76.
37. Alwan HA, van Leeuwen JE. UBPY-mediated epidermal growth factor receptor (EGFR) de-ubiquitination promotes EGFR degradation. *J Biol Chem*. 2007;282:1658–69.
38. Savio MG, Wollscheid N, Cavallaro E, Algisi V, Di Fiore PP, Sigismund S, et al. USP9X controls EGFR fate by deubiquitinating the endocytic adaptor Eps15. *Curr Biol*. 2016;26:173–83.
39. Pareja F, Ferraro DA, Rubin C, Cohen-Dvashi H, Zhang F, Aulmann S, et al. Deubiquitination of EGFR by Cezanne-1 contributes to cancer progression. *Oncogene*. 2012;31:4599–608.
40. Clague MJ, Urbe S. Endocytosis: the DUB version. *Trends Cell Biol*. 2006;16:551–9.
41. Row PE, Prior IA, McCullough J, Clague MJ, Urbe S. The ubiquitin isopeptidase UBPY regulates endosomal ubiquitin dynamics and is essential for receptor down-regulation. *J Biol Chem*. 2006;281:12618–24.
42. Komada M. Controlling receptor downregulation by ubiquitination and deubiquitination. *Curr Drug Discov Technol*. 2008;5:78–84.
43. Ledda F, Paratcha G. Negative regulation of receptor tyrosine kinase (RTK) signaling: a developing field. *Biomark Insights*. 2007;2:45–58.
44. Guo L, Kozlosky CJ, Ericsson LH, Daniel TO, Cerretti DP, Johnson RS. Studies of ligand-induced site-specific phosphorylation of epidermal growth factor receptor. *J Am Soc Mass Spectrom*. 2003;14:1022–31.
45. Perez-Rivas LG, Theodoropoulou M, Ferrau F, Nusser C, Kawaguchi K, Stratakis CA, et al. The gene of the ubiquitin-specific protease 8 is frequently mutated in adenomas causing Cushing's disease. *J Clin Endocrinol Metab*. 2015;100:E997–1004.
46. Meijer IM, Kerperien J, Sotoca AM, van Zoelen EJ, van Leeuwen JE. The Usp8 deubiquitination enzyme is post-translationally modified by tyrosine and serine phosphorylation. *Cell Signal*. 2013;25:919–30.
47. Devarakonda S, Morgensztern D, Govindan R. Genomic alterations in lung adenocarcinoma. *Lancet Oncol*. 2015;16:e342–51.
48. Bansal P, Osman D, Gan GN, Simon GR, Boumber Y. Recent advances in targetable therapeutics in metastatic non-squamous NSCLC. *Front Oncol*. 2016;6:112.
49. Naviglio S, Matteucci C, Matoskova B, Nagase T, Nomura N, Di Fiore PP, et al. UBPY: a growth-regulated human ubiquitin isopeptidase. *EMBO J*. 1998;17:3241–50.
50. Sato T, Shiba-Ishii A, Kim Y, Dai T, Husni RE, Hong J, et al. miR-3941: a novel microRNA that controls IGBP1 expression and is associated with malignant progression of lung adenocarcinoma. *Cancer Sci*. 2017;108:536–42.
51. Travis WD, Brambilla E, Noguchi M, Nicholson AG, Geisinger KR, Yatabe Y, et al. International association for the study of lung cancer/american thoracic society/european respiratory society international multidisciplinary classification of lung adenocarcinoma. *J Thorac Oncol*. 2011;6:244–85.
52. Travis WD, Brambilla E, Nicholson AG, Yatabe Y, Austin JH, Beasley MB, et al. The 2015 world health organization classification of lung tumors: impact of genetic, clinical and radiologic advances since the 2004 classification. *J Thorac Oncol*. 2015;10:1243–60.